Revision 1

LA-Q-ICP-MS apatite U/Pb geochronology using common Pb in plagioclase: examples from layered mafic intrusions

Cora. C. Wohlgemuth-Ueberwasser[1*], Christian Tegner[2], Victoria Pease[1]

[1]PetroTectonics Analytical Facility, Department of Geological Sciences, Stockholm University, 106 91 Stockholm, Sweden, coracwu@gmail.com

[2]Centre of Earth System Petrology, Department of Geoscience, Aarhus University, Denmark

*corresponding author, present address: Helmholtz Centre Potsdam, GFZ German Research Centre for Geosciences, Telegrafenberg, 14473 Potsdam, Germany, phone +49 331 288-1793

Keywords: apatite, feldspar, common Pb, quadrupole ICP-MS, laser ablation

Abstract

Apatite geochronology is a versatile method for providing medium temperature history constraints of magmatic and metamorphic rocks. The LA-ICP-MS technique is widely applied to U/Pb geochronology using a variety of minerals. Apatite U/Pb geochronology, in contrast to e.g. zircon, is compromised by variable amounts of common Pb incorporated into the crystal during growth. Magmatic apatite often shows a sufficient spread in data to obtain a precise and accurate lower intercept age. If this is not the case, the initial Pb isotopic composition needs to be estimated to obtain accurate and precise age information from apatite. Two approaches are common, one being the estimation of common Pb from a Pb evolution model and the other being the measurement of a coexisting mineral phase that tends to incorporate Pb but not U, e.g. feldspar. Most recent studies applying LA-ICP-MS to the

analysis of Pb isotopes in feldspar utilize either multicollector or magnetic sector mass spectrometers. In this study we firstly evaluate the application of quadrupole mass spectrometry for apatite U/Pb geochronology combined with Pb isotopic measurements in feldspar and compare the results with modelled initial Pb isotopic compositions. The resulting age information is accurate and precise despite using plagioclase rather than K-feldspar, as is normally used, to define initial Pb isotope compositions. We apply this method to apatite-bearing gabbroic rocks from layered intrusions (Bushveld, Bjerkreim-Sokndal, Hasvik, and Skaergaard) ranging in age from ca. 2 Ga to ca. 55 Ma and generate metamorphic/cooling ages generally consistent with the known geologic history of these intrusions.

Introduction

Apatite is a valuable mineral for geochronology as it occurs as an accessory mineral in magmatic, sedimentary and metamorphic rocks. In many cases U/Pb ages from apatite agree with zircon in rapidly cooling intrusive rocks (Oosthuyzen and Burger 1973). Nevertheless, substantial differences between U/Pb apatite and zircon ages are observed due to Pb loss or slow cooling (Cliff and Cohen 1980, DeWitt et al. 1984) as the T_C (closure temperature) of zircon and apatite differ significantly, at >900 ºC (Lee et al. 1997) and 450-550 ºC (Cherniak et al. 1991, Chamberlain and Bowring 2000; Schoene and Bowring 2007) or 375 – 570 °C (Cochrane et al. 2014), respectively. The T_C of apatite is dependent on grain size and composition, and is close to the $^{40}Ar/^{39}Ar$ hornblende T_C of c. 550°C (Harrison 1982), and can therefore be used as a medium-temperature thermochronometer. The cooling rate associated with igneous rocks is mainly controlled by size and stagnation depth of an intrusion and may lead to significant differences in the mineral cooling ages.

In contrast to zircon, apatite tends to incorporate not only U but also Pb during crystallization. For this reason U/Pb data need to be corrected for PbC (common Pb) if there is not enough spread in data to derive a lower intercept age in order to obtain accurate ages. This is not only true for the samples analyzed but also for the reference material (Chew et al. 2014). For the PbC correction the initial Pb isotopic composition needs to be established. This can be obtained from the two-stage Pb evolution model of Stacey and Kramers (1975) which is an iterative approach. Alternatively, the initial PbC can be derived from the analysis of the Pb isotopic composition of a paragenetic mineral phase like feldspar that tends to incorporate Pb rather than U and thus records the initial PbC isotopic composition at time of crystallization. In most Pb isotopic studies on feldspar, K-feldspar is used, limiting this technique to evolved samples. It has been considered that plagioclase may incorporate U during crystallization, affecting the $^{207}Pb/^{206}Pb$ ratio. Schwarze and Miller (1968) found 0.004 – 0.030 ppm lattice bound U in K-feldspar and 0.003 – 0.180 ppm in coexisting plagioclase. Nevertheless, Flowerdew et al. (2012) reported high and variable U contents in a K-feldspar sample leading to large uncertainties in $^{207}Pb/^{206}Pb$ initial ratios which might have resulted from partial re-equilibration of Pb isotopes during a late phase of metamorphism. Pb/Pb in feldspar is marked by a T_C of c. 700°C (Cherniak 1995) and can be re-equilibrated during high-grade metamorphic events. Due to the lower T_C of apatite of 375 – 570°C this resetting of the Pb isotopic composition in feldspar would have no or little effect on the accuracy and precision of apatite geochronology.

The accurate and precise in situ analysis of Pb isotopes in feldspar in the literature is mostly limited to SIMS (secondary ion mass spectrometry) and MC-ICP-MS (multi collector-inductively coupled plasma-MS), the latter due to the simultaneous acquisition of Hg and Pb isotopes. This allows for an accurate correction of the ^{204}Hg interference on ^{204}Pb applying natural $^{202}Hg/^{204}Hg$ and / or $^{201}Hg/^{204}Hg$ isotope ratios. This provides accurate and precise $^{208}Pb/^{204}Pb$, $^{207}Pb/^{204}Pb$, and $^{206}Pb/^{204}Pb$ ratios as usually applied in traditional Pb isotopic studies (e.g. Tyrrell et al. 2007, 2010). The PbC correction in apatite geochronology only requires the $^{207}Pb/^{206}Pb$ ratio, which might be possible to acquire by LA-Q-ICP-MS (laser ablation-quadrupole-ICP-MS) at a sufficient accuracy and precision. Chew et al. (2011) validated the LA-ICP-MS method using apatite with initial PbC from feldspar applying a magnetic sector MS which has a significantly higher sensitivity than quadrupole ICP-MS and produces better precision due to the simultaneous detection of the isotopes. Therefore we present a new and unconventional approach using the Pb isotopic composition of feldspar obtained from LA-Q-ICP-MS for the PbC correction of apatite U/Pb ages. Following the evaluation of analytical parameters, accuracy and precision of this approach, we present analyses of five samples from four layered intrusions that have previously been dated by e.g. U/Pb in zircon or Sm/Nd mineral/whole rock as a test of the method.

Samples

Pre-analyzed feldspar

Three feldspar samples with established Pb isotopic compositions (Table 1) have been analyzed to validate the accuracy and precision of Pb isotope analyses of feldspar. The samples are from the Antarctic and comprise one granite from Cole Peninsula (R414.1) and one granite gneiss each from Heimefrontfjella (Z332.1) and Read Mountains (sample Z.1098.6). They have previously been analyzed for Pb isotopes using the solution MC-ICP-MS method (Flowerdew et al. 2012).

Apatite standards

Within this study a series of reference materials for apatite geochronology have been measured against each other to constrain optimum analytical conditions and verify the method applied (Table 1). They cover a range of ages from 31.44 Ma (Durango; McDowell et al. 2005) to 377.5 Ma (Kovdor; Amelin and Zaitsev 2002) and 523.5 Ma (Mount McClure;

Schoene and Bowring 2006). The external standard for all apatite analyses was Madagascar apatite with 474 Ma (Thomsen et al. 2012).

<u>Apatite and feldspar from intrusions</u>

Furthermore, five samples from four different layered intrusions were crushed, milled and separated via Wilfley shaking table and hand magnet for apatite and plagioclase feldspar (Table 2). Grains were handpicked and mounted in 2.5 cm epoxy pucks. To evaluate the analytical approach of combining Pb isotopic data from LA-Q-ICP-MS with apatite geochronology it was compared to accuracy and precision of apatite ages derived by initial PbC calculation after Stacey and Kramers (1975).

Sample 90-22-467 was derived from the Skaergaard Intrusion (East Greenland). The Skaergaard Intrusion was formed at 55.96 Ma based on U/Pb zircon CA-TIMS (chemical abrasion-thermal ionization MS) of ferrodiorite (Wotzlaw et al. 2012) and is a shallow level intrusion that fractionated as a closed system. Sample 90-22-467 is part of drill core 90-22 and originates from the Upper Zone b whose base is marked by the appearance of abundant apatite (Tegner, 1997).

Two samples originate from the Hasvik Layered Intrusion (Norway). The gabbroic Hasvik Layered Intrusion is part of the Seiland Igneous Province within the North Norwegian Caledonides and has been emplaced in the middle crust at 6 – 8 kbar (H. Reginiussen, Ph.D. thesis, Univ. Tromsø, 1996). It is supposed to have experienced upper greenschist facies metamorphism at 425 – 415 Ma as indicated by Ar/Ar dating of muscovite and hornblende minerals (Dallmeyer 1988). Samples CT-40 and 03N17 from this study originate from the Upper Zone which is the uppermost portion of the Layered Series and consists of oxide-apatite ferronorites (Tegner et al. 1999). Daly et al. (1991) reported a Sm/Nd mineral/whole rock age of 700 ± 33 Ma, while ID-TIMS (isotope dilution-TIMS) U/Pb zircon data suggest a crystallization age of 562 ± 6 Ma (Roberts et al. 2006).

One sample (NH-17) has been part of the Bjerkreim-Sokndal Intrusion (Norway). Bjerkreim-Sokndal Intrusion has a published ID-TIMS U/Pb age of 932 ± 5 Ma from the Bjerkreim-Sokndal quartz mangerite (Pasteels et al. 1979). The intrusion consists of a series of 6 mega-cyclic units (MCU) and formed at pressures of 4 – 6 kbar (Auwera and Longhi 1994). Sample NH-17 originates from the eastern flank of the Bjerkreim-lobe in the upper part of MCU III (Meyer et al. 2002).

The oldest sample for this study comes from the Bushveld Complex (South Africa). The Bushveld complex is a mafic intrusion with an age of 2056.88 ± 0.41 Ma (U–Pb zircon CA-TIMS age of pegmatitic orthopyroxenite; Scoates and Wall 2015). The accretion and crystallization of the mafic Bushveld Complex was extremely rapid and can be bracketed between an U-Pb zircon age of 2055.91 ± 0.26 Ma at the chilled base and 2054.89 ± 0.37 Ma from a pyroxenite in the central part of the intrusion (Zeh et al. 2015). The ages are consistent with thermal modeling (Cawthorn and Walraven 1998). Thermal modeling further suggests rapid cooling through 700°C in less than a million years (Zeh et al. 2015), consistent with constraints from rutile ages (Scoates and Wall 2015). At ~2 Ga it experienced a hydrothermal event as indicated by $^{40}Ar/^{39}Ar$ biotite ages of 1999 ± 10 Ma and 2002 ± 10 Ma (Scoates and Wall 2015). Sample 1w1423.4 is from the Bierkraal drill core from Upper Zone c which marks the appearance of apatite (Tegner et al. 2006). Zeh et al. (2015) obtained an U–Pb age of 2055.81 ± 0.76 Ma for zircon of the Upper Zone.

Methods

All analyses were carried out with a New Wave NWR-193 excimer laser ablation system coupled to a Thermo XSeries2 quadrupole ICP-MS at the PetroTectonics Analytical Facility at the Department of Geological Sciences, Stockholm University. Analytical conditions are given in Table 3. Prior to analysis the instrument was tuned to high sensitivity while keeping the ThO/Th production rate below 0.5%.

Apatite

For apatite U/Pb geochronology each analysis comprised 15 s background, 30 s analysis, 10 s wash-out. Ablation was carried out with 50 µm spot size, laser energy density of 7 J cm^{-2}, and a repetition rate of 10 Hz. Each reference material used as unknown for method establishment was analyzed 15 times and each sample from the layered intrusions 15 to 31 times. External standardization was performed using Madagascar apatite, analyzed at the start and end of the analytical sequence and bracketing 10 analyses of the samples. Mount McClure was analyzed together with the samples and treated as unknown to control the "within-run" accuracy and yielded a ^{207}Pb-corrected age of 523.6 ± 2.5 Ma (n=18).

Analyzed isotopes are given in Table 4. Three different settings for dwell times were used in order to verify the accuracy and precision that can be achieved with this instrumentation. Data from the instrument was processed using the VizualAge_UComPbine DRS (data reduction scheme; Chew et al. 2014) within Iolite (Hellstrom et al. 2008; Paton et al. 2011). It allows for PbC correction of the external standard before correction for downhole fractionation and instrument drift, in this study the ^{207}Pb correction method. The initial ^{207}Pb/^{206}Pb isotopic compositions of reference materials analyzed as samples in this study are taken from the literature (Table 1). For the unknowns data processing was carried out with Pb isotopic compositions calculated from the Stacey and Kramers (1975) Pb evolution model as well as with the Pb isotopic composition derived from analyses of coexisting plagioclase feldspar.

Feldspar

Pb-isotopes in feldspar have been analyzed with a maximum spot diameter of 150 µm, laser energy density of 8 J cm^{-2}, laser frequency of 20 Hz, and raster speed of 5 µm s^{-1}. Each analysis comprised 30 seconds of gas blank and 30 seconds wash-out. Two line analyses each were conducted on NIST 610, 612, and 614 as external standard with a length of 300µm. Instrument tuning was focused on high sensitivity (> 10000 cps/ppm on ^{207}Pb) with ThO/Th of <0.5%. The analyzed isotopes were ^{200}Hg, ^{201}Hg, ^{202}Hg, ^{203}Tl, ^{204}Hg-Pb, ^{205}Tl, ^{206}Pb, ^{207}Pb, and ^{208}Pb.

Data processing was performed with Excel using raw data from the analyses. It included background subtraction for each isotope and monitoring isotopic fractionation by calculating fractionation factors for each spectrum after Fryer et al. (1995). No outliers were rejected and $^{207}Pb/^{206}Pb$ ratios were calculated as ratios from averages of background subtracted cps over the complete raster analyses. Additionally, the deviation of measured versus published Pb isotope ratios of 0.38% in NIST 612 was used to correct the Pb isotopes of the samples. There was no need to correct for instrument drift as $^{207}Pb/^{206}Pb$ ratios were stable during the analytical session (Figure 1). Each sample was analyzed 15 times and averaged.

Results

Apatite standards

For the apatite reference materials ages were calculated as ^{207}Pb-corrected ages (Chew et al. 2014). The highest accuracy and precision was obtained with the longest dwell times (Table 5). The precision for the Durango sample is slightly lower than for Kovdor and Mount McClure (2.58%; Figure 2). This can be attributed to lower count rates on ^{207}Pb with ~700 cps in contrast to Mount McClure with ~1000 cps and Kovdor with ~4000 cps. Accuracy and precision for Mount McClure are high with 0.06% and 0.78%, respectively. Analyses of

Kovdor apatite yields lower accuracy and precision of 0.26% and 1.06%, respectively, which might be related to more heterogeneous U and Pb distribution. The precision was improved by increasing the number of analyses to 30, resulting in an accuracy of 0.19% and precision of 0.89%.

Pre-analyzed feldspar

To validate the successful set-up of the feldspar method with respect to accuracy and precision, three K-feldspar samples previously analyzed by Flowerdew et al. (2012) were analyzed within this study (Table A1). From analyses of NIST 610, 612, and 614 we conclude that NIST614 with 2.3 ppm Pb does not give accurate $^{207}Pb/^{206}Pb$ isotope ratios on our analytical setup. The same is true for NIST612 with a Pb concentration of 39 ppm (precision 0.5%, n=12). NIST 610 is heterogeneous with respect to $^{207}Pb/^{206}Pb$ isotope ratios with a precision of 1 % (n=12). NIST612 yielded a higher precision of 0.2% (n=12) and was applied as external standard for further analyses. All feldspar analyses yielded fractionation factors (after Fryer et al. 1995) of 1.0, i.e.- no downhole isotopic fractionation was observed (Table 6). The comparison of the acquired LA-Q-ICP-MS isotope ratios with published values shows that they are in good agreement (Figure 3). Compared to solution MC-ICP-MS, the 2 σ errors are larger (Table 6).

We found the U concentration in the analyzed feldspars below the detection limit of our instrument at~0.05 ppm. Thus we are not able to correct for effects of initial U in-growth.

Feldspar and apatite from intrusions

$^{207}Pb/^{206}Pb$ ratios from feldspar (andesine composition) analyses for sample 90-22-467 from the Skaergaard intrusion are significantly higher than those derived from the Stacey and Kramers model with 0.8851 compared to 0.8387. Apatite analyses yield a ^{207}Pb-corrected age of 55.35 ± 6.6 Ma, applying a PbC correction with initial PbC derived from feldspar analyses. Applying a Stacey and Kramers initial PbC yields a ^{207}Pb-corrected age of 55.69 ± 5.9 Ma (Table 7, Figure 4). Both ages are close to the Tera-Wasserburg intercept age of 58 ± 19 Ma but are more precise (Figure 5). Analyses of Durango apatite with the youngest crystallization age among the reference materials and Skaergaard apatite show that there is no limitation of the method towards younger intrusions.

Samples from the Hasvik layered intrusion also show significant differences in PbC composition comparing ^{207}Pb/^{206}Pb ratios from feldspar (labradorite composition) analyses and from the Stacey and Kramers calculation (Table 7; Figure 4 A and B). The ^{207}Pb-corrected ages from both initial PbC compositions overlap within error with 424.7 ± 4.7 Ma (03N17; feldspar) and 434.5 ± 6.1 Ma (03N17; S & K), and 422.7 ± 5.5 Ma (CT40; feldspar) and 422.6 ± 5.8 Ma (CT40; S & K). Interestingly, the ages of both samples are significantly younger than previously reported zircon U/Pb ages of 562 ± 6 Ma (Roberts et al. 2006). They agree well with ^{40}Ar/^{39}Ar hornblende and muscovite ages of 425 – 415 Ma (Dallmeyer 1988).

Feldspar (andesine composition) from the Bjerkreim-Sokndal Intrusion (NH-17) has a ^{207}Pb/^{206}Pb ratio of 0.8716, slightly lower than the Stacey and Kramers calculated ratio of 0.8970. ^{207}Pb-corrected apatite ages overlap within error with 906 ± 7.8 Ma and 907.7 ± 8 Ma (Table 7; Figure 4 C). These are both significantly younger than the published zircon age of 932.5 ± 6 Ma (Figure 6), in keeping with the lower Tc of apatite.

Initial Pb isotope ratios of the Bushveld sample as derived from feldspar (labradorite composition) analyses (1.0029) and the Stacey and Kramers calculation (1.0059) are in good agreement. Correspondingly, the ^{207}Pb-corrected ages are close to each other (2056 ± 7.8 Ma and 2056.2 ± 9 Ma; Table 7; Figure 4 D) and to the published zircon age of 2056.88 Ma (Figure 6).

Discussion

Apatite geochronology of sample 90-22-467 from the Skaergaard intrusion produced ages with good accuracy and precision using either the initial PbC from feldspar analyses or PbC from the Stacey and Kramers model. The least precise ages are obtained by calculating a lower intercept age from uncorrected $^{207}Pb/^{206}Pb$ and $^{238}U/^{206}Pb$ ratios anchored at initial PbC (Figure 5, Table 7). The application of initial PbC from feldspar analyses yielded an intercept age of 58 ± 19 Ma whereas the Stacey and Kramers PbC composition gave an age of 35 ± 14 Ma; both ages have low accuracy and precision. Considering the ^{206}Pb, ^{207}Pb, and ^{238}U count rates (cps) of apatite (Table 8), the sample from the Skaergaard intrusion has the lowest Pb and U concentration among the different analyzed samples. Nevertheless, analyses of Durango apatite (31.44 Ma) yielded ^{206}Pb and ^{207}Pb cps of only 200 cps and 40 cps, respectively, but significantly higher ^{238}U cps of 28000 (compared to 2000 in sample 90-22-467). Therefore, the accuracy and precision of ages for young samples is not only controlled by Pb and U concentration but also by the spread in radiogenic Pb/common Pb ratios. In contrast, ^{207}Pb corrected ages of 55.35 ± 6.6 Ma (feldspar) and 55.69 ± 5.9 Ma (Stacey and Kramers) are accurate and precise, and agree well with the accepted crystallization age of ca. 56 Ma (Zeh et al. 2015).

^{207}Pb-corrected ages of the two samples from the Hasvik Intrusion agree well with ~423 Ma (CT-40) and ~425 Ma (NH17; Table 7). PbC anchored Tera-Wasserburg ages of both samples are in agreement, independent of which initial PbC (from feldspar or from Stacey and Kramers) is applied (Figure 5). Sample CT-40 yields intercept ages of 423.7 ± 8.5 Ma (feldspar) and 432.6 ± 5.4 Ma (Stacey and Kramers), sample 03N17 ages of 422.3 ± 8.6 Ma (feldspar) and 432.6 ± 5.2 (Stacey and Kramers). This age range (422 – 433 Ma) correlates within error with Ar/Ar hornblende and muscovite ages of 425 – 415 Ma (Dallmeyer 1988; Figure 6) and with the main phase of Caledonian orogenesis at 425 – 400 Ma (e.g. Gee 1982).

This orogeny might have caused Pb loss in apatite and reset the thermochronometer, which then indicates peak metamorphic temperatures above the apatite T_C of 375 to 570ºC. The Pb isotope system might also have been reset during this metamorphic event.

Anchored Tera-Wasserburg intercept ages of sample NH17 from the Bjerkreim-Sokndal intrusion are in good agreement with the ^{207}Pb-corrected ages of 906 ± 11 Ma (feldspar) and 904.7 ± 8.1 Ma (Stacey and Kramers). The apatite age strongly differs from the published zircon age of 932 Ma which can be explained by slow cooling of the intrusion of ~20°C/Ma, assuming an apatite T_C of 450°C. This is supported by a paleomagnetic study arguing the remenent magnetism was acquired at 900 Ma due to slow cooling (Brown and McEnroe, 2004). Despite this concise cooling path Rb/Sr whole rock analyses yielded an age of 857 ± 21 Ma (Pasteels et al., 1979). The high T_C of c. 700°C for Rb/Sr should have also reset the U/Pb apatite and Pb/Pb feldspar ratios which has not been observed within this study. Kagami et al. (2003) reported lowering of the Rb/Sr T_C down to c. 400°C in presence of fluids. Lowering the T_C of the Rb/Sr system to 400°C leads to a coherent cooling history for the Bjerkreim-Sokndal intrusion.

For the previously described samples, the anchored Tera-Wasserburg ages were in agreement with sample ages (Hasvik) and initial PbC (Bjerkreim-Sokndal). In contrast, intercept ages for the Bushveld complex (sample 1w1423.4) yield older ages of 2108 ± 34 Ma (feldspar) and 2109 ± 33 Ma (Stacey and Kramers) that do not overlap with the published age of 2055.88 Ma. This inaccuracy is related to the limited spread in radiogenic Pb/common Pb ratios (Figure 5). Nevertheless, ^{207}Pb corrected ages of 2056 ± 7.8 Ma and 2056.2 ± 9 Ma agree well the published zircon U/Pb age of 2056.88 Ma.

We conclude that the deviation between measured versus calculated initial PbC is not related to application of LA-Q-ICP-MS, but to the analyses of plagioclase feldspar in contrast to K-feldspar from earlier studies. Any analysis of pre-analyzed K-feldspar produced accurate results with deviations of measured to published values below 0.8% (Table 6). These samples yielded raw cps on ^{206}Pb and ^{207}Pb >100000, significantly higher than count rates for the plagioclase of the samples (Table 8). Therefore the mostly lower ^{207}Pb/^{206}Pb ratios of the newly analyzed samples are related to low Pb count rates for these feldspar compositions. This might either reflect a general depletion of the host magma in Pb crystallizing plagioclase compared to Na-K-feldspar or different partition coefficients for Pb silicate melt/K-Na-feldspar and silicate melt/plagioclase. It is noteworthy that LA-Q-ICP-MS of apatite allows for the reliable geochronology of cooling events (Skaergaard, Bjerkreim-Sokndal, and Bushveld intrusions) and metamorphic events (Hasvik intrusion). In the latter case, the T_C of 375 – 570°C for U/Pb in apatite allows to estimate minimum peak metamorphic temperatures.

Implications

- LA-Q-ICP-MS for apatite U/Pb geochronology produces precise and accurate data, independent of the method applied for initial PbC – feldspar analyses or the Stacey and Kramers calculation. Accuracy and precision of Pb isotope analyses in plagioclase is sufficient for PbC correction with the application of quadrupole mass spectrometry.
- Analyses of feldspar for initial PbC is compromised by the feldspar composition. While measured Pb isotopes in K-feldspar are accurate at < 0.8% deviation from published values, analyses of plagioclase show a deviation from Stacey and Kramers model composition.
- Although measured initial PbC and calculated PbC deviate, neither the ^{207}Pb-corrected age nor the anchored Tera-Wasserburg intercept age is affected and ages for the different initial PbC overlap within error.
- Intercept ages of young samples like 90-22-467 from the Skaergaard intrusion can be compromised by a limited spread of radiogenic Pb/common Pb ratios. Nevertheless, it

should be noted that the analytical technique is not limited to samples older than this (56 Ma) as we could produce an accurate and precise age for the Durango apatite (31 Ma).

Acknowledgements

The PetroTectonics Analytical Facility was established with funding from the Knut and Alice Wallenberg Foundation. M. Flowerdew is gratefully thanked for providing the feldspar samples. Henrik Schillerup and Gurli Meyer are gratefully thanked for providing sample NH17. CT acknowledges funding from the Danish National Research Foundation and VP from the Swedish Research Council. J. Hanchar, S. Thomson, D. Chew and M. Whitehouse are acknowledged for providing apatite reference materials for this study. D. Chew and M. Flowerdew are highly acknowledged for thorough reviews that led to vast improvements of the manuscript.

References

Amelin, Y. and Zaitsev, A.N. (2002) Precise geochronology of phoscorites and carbonatites: The critical role of U-series disequilibrium in age interpretations. Geochimica et Cosmochimica Acta, 66, 2399–2419.

Auwera, J.V. and Longhi, J. (1994) Experimental study of a jotunite (hypersthene monzodiorite): constraints on the parent magma composition and crystallization conditions (P, T, f_{O2}) of the Bjerkreim-Sokndal layered intrusion (Norway). Contributions to Mineralogy and Petrology, 118, 60-78.

Brown, L. L. and McEnroe, S. A. (2004) Paleomagnetism of the Egersund–Ogna anorthosite, Rogaland, Norway, and the position of Fennoscandia in the Late Proterozoic. Geophysical Journal International, 158, 479–488.

Cawthorn, R. G. and Walraven, F. (1998) Emplacement and crystallization time for the Bushveld Complex. Journal of Petrology, 39, 1669-1687.

Chamberlain, K.R. and Bowring, S.A. (2000) Apatite–Feldspar U–Pb thermochronometer: A reliable, mid-range (450 °C), diffusion-controlled system. Chemical Geology, 172, 173–200.

Cherniak, D. J. (1995) Diffusion of Pb plagioclase and K feldspar: an investigation using Rutherford backscattering and resonant nuclear reaction analysis. Contributions to Mineralogy and Petrology, 120, 358–371.

Cherniak, D. J., Lanford, W. A., and Ryerson, F. J. (1991) Lead diffusion in apatite and zircon using ion implantation and Rutherford Backscattering techniques. Geochimica et Cosmochimica Acta, 55, 1663–1673.

Chew, D.M., Sylvester, P.J. and Tubrett, M.N. (2011) U-Pb and Th-Pb dating of apatite by LA-ICPMS. Chemical Geology, 280, 200-216.

Chew, D., Petrus, J., and Kamber, B. (2014) U–Pb LA–ICPMS dating using accessory mineral standards with variable common Pb. Chemical Geology, 363, 185–199.

Cliff, R. A., and Cohen, A. (1980) Uranium–Lead isotope systematics in a regionally metamorphosed tonalite from the eastern Alps. Earth and Planetary Science Letters, 50, 211–218.

Cochrane, R., Spikings, R.A., Chew, D., Wotzlaw, J.-F., Chiaradia, M., Tyrrell, S., Schaltegger, U. and Van der Lelij, R. (2014) High temperature (>350 °C) thermochronology and mechanisms of Pb loss in apatite. Geochimica et Cosmochimica Acta, 127, 39-56.

Dallmeyer, R. D. (1988) Polyorogenic 40Ar/39Ar mineral age record within the Kalak Nappe Complex, Northern Scandinavian Caledonides. Journal of the Geological Society, London, 145, 705-716.

Daly, J. S., Aitcheson, S. J., Cliff, R. A., Gayer, R. A., and Rice, H. N (1991) Geochronological evidence from discordant plutons for a late Proterozoic orogen in the Caledonides of Finnmark, northern Norway. Journal of the Geological Society, London, 148, 29–40.

DeWitt, E., Armstrong, R. L., Sutter, J. F., and Zartman, R. E. (1984) U–Th–Pb, Rb–Sr, and Ar–Ar mineral and whole rock isotopic systematics in a metamorphosed granitic terrane, southeastern California. Geological Society of America Bulletin, 95, 723–739.

Flowerdew, M., Tyrrell, S., Riley, T., Whitehouse, M., Mulvaney, R., Leat, P., and Marschall, H. (2012) Distinguishing East and West Antarctic sediment sources using the Pb isotope composition of detrital K-feldspar. Chemical Geology, 292, 88-102.

Fryer, B. J., Jackson, S. E., and Longerich, H. P. (1995) The design, operation and role of the laser-ablation microprobe coupled with an inductively coupled plasma-mass spectrometer (LAM-ICP-MS) in the Earth Sciences. Canadian Mineralogist, 33, 303–312.

Gee, D.G. (1982) The Scandinavian Caledonides, Terra Cognita, 2, 89–96.

Harrison, T.M. (1982) Diffusion of 40Ar in hornblende. Contributions to Mineralogy and Petrology, 78, 324–331.

Hellstrom, J., Paton, C., Woodhead, J., and Hergt J. (2008) Iolite: Software for spatially resolved LA- (quad and MC) ICPMS analysis. In P. Sylvester, Ed, Laser Ablation ICP–MS in the Earth Sciences: Current Practices and Outstanding Issues, Mineralogical Association of Canada, Quebec, Canada, p. 343–348.

Kagami, K., Shimura, T., Yuhara, M., Owada, M., Osanai, Y. and Shiraishi, K. (2003) Resetting and closing condition of Rb-Sr whole-rock isochron system: some samples of metamorphic and granitic rocks from the Gondwana super-continent and Japan Arc. Polar Geoscience, 16, 227-242

Lee, J. K. W., Williams, I. S., and Ellis, D. J. (1997) Pb, U and Th diffusion in natural zircon. Nature, 390, 159-162.

McDowell. F. W., McIntosh. W. C.. and Farley K. A. (2005) A precise Ar-40–Ar-39 reference age for the Durango apatite (U–Th)/He and fission-track dating standard. Chemical Geology, 214, 249–263.

Meyer, G. B., Schiellerup, H., and Tegner, C. (2002) Chemical characterization of ilmenite, magnetite and apatite in the Bjerkreim-Sokndal Layered Intrusion, Rogaland, South Norway. Report 2002.042, Geological Survey of Norway.

Mezger, K., Hanson, G.N., and Bohlen, S.R. (1989) High-precision U-Pb ages of metamorphic rutile: application to the cooling history of high-grade terranes: Earth and Planetary Science Letters, 96,106-118.

Mezger, K., Essene, E. J., Halliday, A. N. (1992) Closure temperatures of the Sm-Nd system in metamorphic garnets. Earth and Planetary Science Letters, 113,397-409.

Oosthuyzen, E. J., and Burger, A.J. (1973) The suitability of apatite as an age indicator by the uranium–lead isotope method. Earth and Planetary Science Letters, 18, 29–36.

Pasteels, P., Demaiffe, D., and Michot, J. (1979) U–Pb and Rb–Sr geochronology of the eastern part of the south Rogaland igneous complex, southern Norway. Lithos. 12, 199–*208.*

Paton, C., Hellstrom, J.C., Paul, B., Woodhead, J.D., and Hergt J.M. (2011) Iolite: Freeware for the visualisation and processing of mass spectrometric data. Journal of Analytical Atomic Spectrometry, 26, 2508-2518.

Purdy, J.W. and Jäger, E. (1976) K-Ar ages on rock-forming minerals from the Central Alps. Memoirs of the Institute of Geology and Mineralogy of the University of Padova 30,31 p.

Roberts, R. J., Corfu, F, Torsvik T. H., Ashwal L. D., and Ramsay D. M. (2006) Short-lived mafic magmatism at 560-570 Ma in the northern Norwegian Caledonides: U/Pb zircon ages from the Seiland Igneous Province. Geological Magazine, 143, 887-903.

Schoene, B., and Bowring S.A. (2006) U–Pb systematics of the McClure Mountain syenite: thermochronological constraints on the age of the Ar-40/Ar-39 standard MMhb. Contributions to Mineralogy and Petrology, 151, 615–630.

Schoene, B., and Bowring, S.A. (2007) Determining accurate temperature–time paths from U–Pb thermochronology: An example from the Kaapvaal craton, southern Africa. Geochimica et Cosmochimica Acta, 71, 165–185.

Schwarze, R. R., and Miller, D. S. (1968) Uranium distribution between coexisting feldspars from selected pegmatites by fission track method. Transactions American Geophysical Union, 49, 334.

Scoates, J. S., and Wall, C. J. (2015) Geochronology of Layered Intrusions. In B. Charlier et al. (Eds): Layered Instrusions, Springer Geology, p. 3-74.

Stacey, J.S., and Kramers, J.D. (1975) Approximation of terrestrial lead isotope evolution by a two-stage model. Earth and Planetary Science Letters, 26, 207–221.

Tegner, C. (1997) Iron in plagioclase as a monitor of the differentiation of the Skaergaard intrusion. Contributions to Mineralogy and Petrology, 128, 45–51.

Tegner, C., Robins, B., Reginiussen, H., and Grundvig, S. (1999) Assimilation of crustal xenoliths in a basaltic magma chamber: Sr and Nd isotopic constraints from the Hasvik Layered Intrusion, Norway. Journal of Petrology, 40, 363–80.

Tegner, C., Cawthorn, R.G., and Kruger, F.J. (2006) Cyclicity in the Main and Upper Zones of the Bushveld Complex, South Africa: crystallization from a zoned magma sheet. Journal of Petrology, 47, 2257-2279.

Thomson, S. N., Gehrels, G. E., Ruiz, J., and Buchwaldt R. (2012) Routine low-damage apatite U–Pb dating using laser ablation multicollector-ICPMS. Geochemistry Geophysics Geosystems, 13, Q0AA21.

Tyrrell, S., Haughton, P. D. W., and Daly, J. S. (2007) Drainage reorganization during breakup of Pangea revealed by in-situ Pb isotopic analysis of detrital K-feldspar. Geology, 35, 971-974.

Tyrrell, S., Souders, A. K., Haughton, P. D. W., Daly, J. S., and Shannon, P. M. (2010) Sedimentology, sandstone provenance and palaeodrainage on the eastern Rockall Basin margin: evidence from the Pb isotopic composition of detrital K-feldspar. Geological Society, London, Petroleum Geology Conference series, 7, 937-952.

Wotzlaw, J. F., Bindeman, I. N., Schaltegger, U., Brooks, C.,K., and Naslund, H.R. (2012) High-resolution insights into episodes of crystallization, hydrothermal alteration and remelting in the Skaergaard intrusive complex. Earth and Planetary Science Letters, 355-356, 199-212.

Zeh, A., Ovtcharova, M., Wilson, A. H. and Schaltegger, U. (2015) The Bushveld Complex was emplaced and cooled in less than one million years – results of zirconology, and geotectonic implications. Earth and Planetary Science Letters, 418, 103–114.

Figures and tables

Figure 1: Variation of $^{207}Pb/^{206}Pb$ isotope ratios in NIST 612 over an analytical session.

Figure 2: Diagrams showing the ^{207}Pb-corrected ages for Durango, Mount McClure and Kovdor apatites analyzed with Madagascar apatite as external standard.

Figure 3: Comparison of ^{207}Pb/^{206}Pb isotope ratios from published solution MC-ICP-MS values (Flowerdew et al., 2012) with measured values. Errors are 2 sigma, errors of MC-ICP-MS values are within in the symbol. The ratios are within error of the 1:1 correlation line.

Figure 4: ^{207}Pb-corrected ages of the samples from the Hasvik, Bjerkreim-Sokndal, Bushveld, and Skaergaard intrusions calculated with PbC from feldspar analyses. A: CT40; B: 03N17; C: NH17; D: 1w1423.4; E: 90-22-467. Filled symbols are rejected data points (2-sigma outlier rejection in UComPbine) and not included in the ^{207}Pb-corrected age calculation.

Figure 5: Tera-Wasserburg diagrams for the samples anchored through initial PbC as derived from feldspar analyses.

Figure 6: Temperature-age (^{207}Pb corrected) relations of the four investigated intrusions. A: Bjerkreim-Sokndal, B: Hasvik, C: Bushveld, D: Skaergaard; blue: zircon T_C > 900°C (Lee et al. 1997), orange: Rb/Sr whole rock T_C 700°C (Kagami et al. 2003), green: Sm/Nd whole rock T_C 600 ± 30°C (Mezger et al. 1992), yellow: Ar/Ar hornblende T_C 550°C (Harrison 1982), red: Ar/Ar muscovite T_C 400°C (Purdy and Jäger 1976), violet: rutile T_C 400-450°C (Mezger et al. 1989), dotted: apatite T_C 375- 570°C (Cherniak et al. 1991, Chamberlain and Bowring 2000, Schoene and Bowring 2007, Cochrane et al. 2014). Ages other than apatite ages from this study (grey boxes) are indicated with numbers: 1) Pasteels 1979; 2) Roberts et

al. 2006; 3) Daly et al. 1991; 4) Dallmeyer 1988; 5) Zeh et al. 2015; 6) Scoates and Wall 2015; 7) Wotzlaw et al. 2012.

*Table 1: Reference materials and feldspar samples applied in this study for apatite U/Pb ages and PbC composition in feldspar (*calculated from published $^{207}Pb/^{204}Pb$ – $^{206}Pb/^{204}Pb$ ratios).*

Table 2: Samples analyzed in this study for apatite U/Pb ages and Pb isotopic composition in feldspar.

Table 3: Instrumental parameters and analytical conditions of the LA-ICP-MS system applied for quantitative analyses.

Table 4: Instrument dwell times for U/Pb geochronology of apatite.

Table 5: ^{207}Pb-corrected ages for apatite reference materials analyzed as unknowns.

Table 6: $^{207}Pb/^{206}Pb$ ratios of the pre-analyzed samples in comparison with published values and the deviation of measured from published values in %.

Table 7: $^{207}Pb/^{206}Pb$ ratios from feldspar analyses and from Stacey and Kramers Pb evolution model (S & K) with corresponding ^{207}Pb-corrected ages of analyzed apatite samples.

Table 8: Raw count rates in counts per second (cps) for 206Pb, 207Pb, and 238 Uin apatite and feldspar.

(DOI will not work until issue is live.) DOI: http://dx.doi.org/10.2138/am-2017-5903

Appendices:

Table A1: ^{207}Pb/^{206}Pb ratios of spot analyses of pre-analyzed feldspar grains and unknowns with fractionation factors (FF) calculated after Fryer et al. (1995) and U concentration from LA-ICP-MS. Note: detection limit is 0.05 ppm. Corr. NIST612: corrected for difference between published and measured 207/206 in NIST612.

Table A2: ^{207}Pb-corrected ages for spot analyses on apatite applying PbC from feldspar and Stacey and Kramers (S & K) and ^{207}Pb/^{206}Pb as well as ^{238}U/206Pb ratios with corresponding error correlation as used for anchored Tera-Wasserburg diagrams.

This is a preprint, the final version is subject to change, of the American Mineralogist (MSA)
Cite as Authors (Year) Title. American Mineralogist, in press.
(DOI will not work until issue is live.) DOI: http://dx.doi.org/10.2138/am-2017-5903

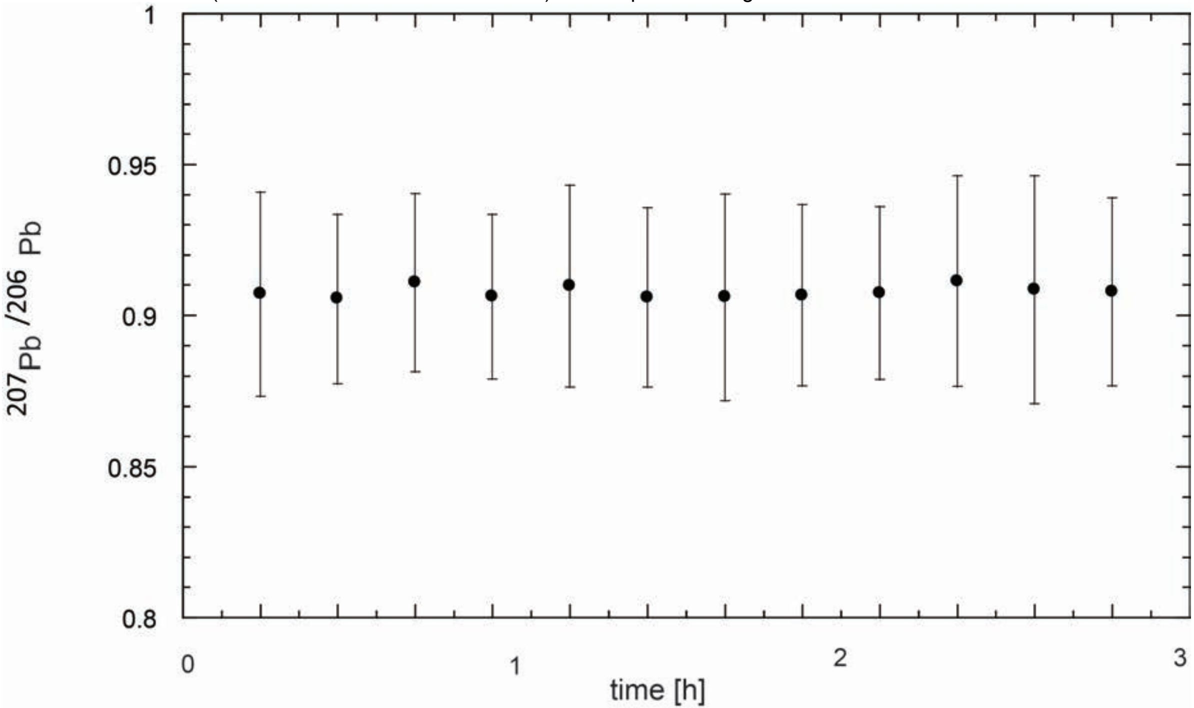

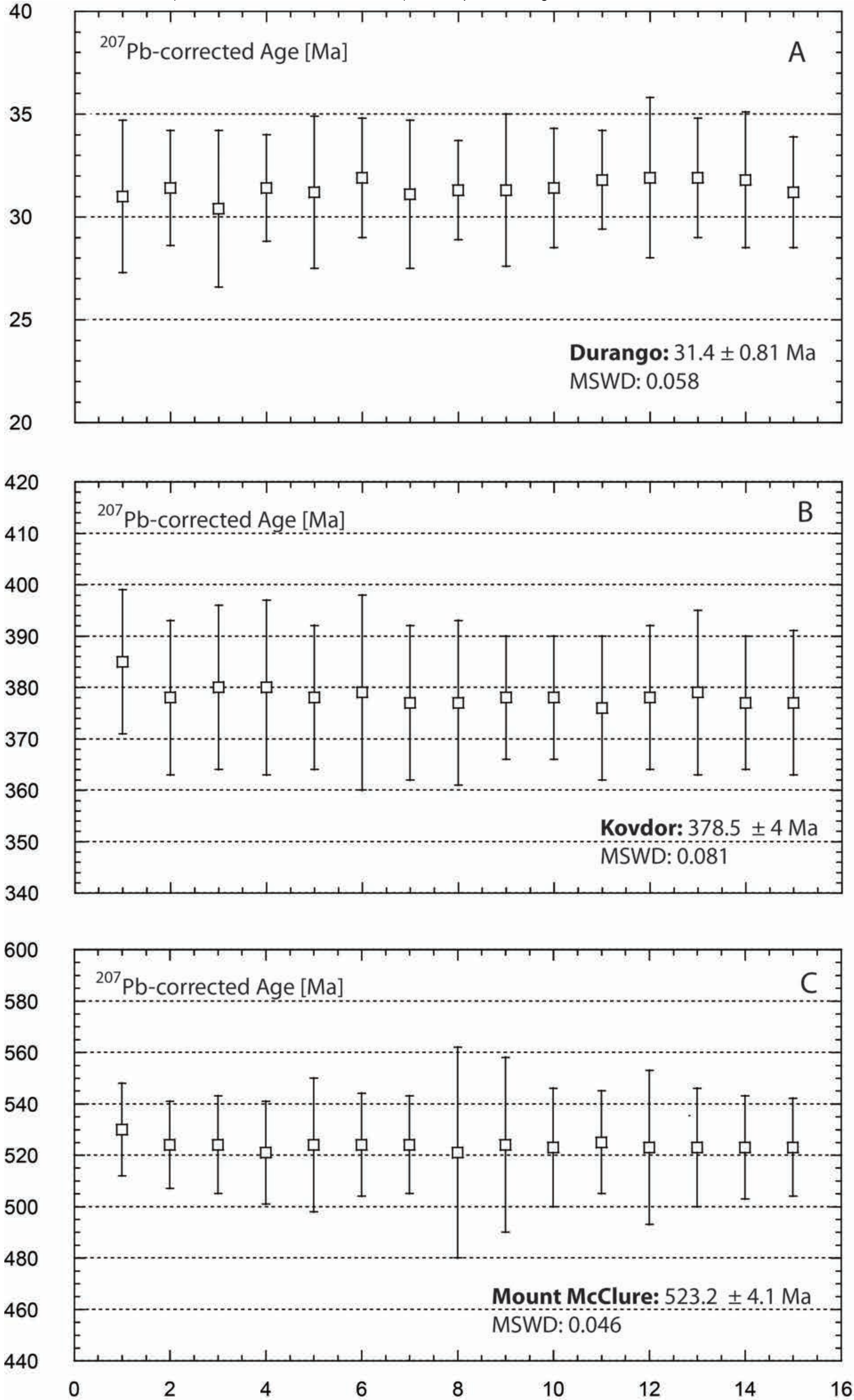
207Pb-corrected Age [Ma]
A
Durango: 31.4 ± 0.81 Ma
MSWD: 0.058
207Pb-corrected Age [Ma]
B
Kovdor: 378.5 ± 4 Ma
MSWD: 0.081
207Pb-corrected Age [Ma]
C
Mount McClure: 523.2 ± 4.1 Ma
MSWD: 0.046

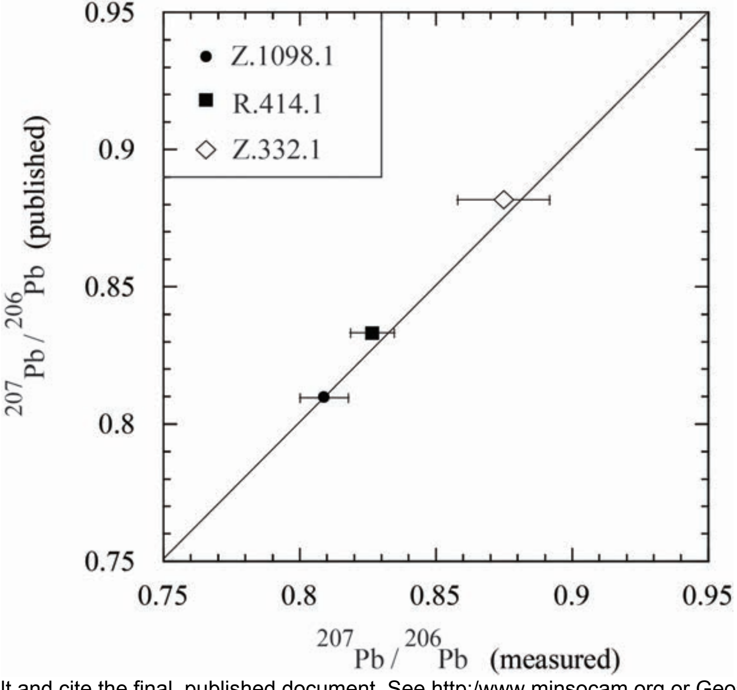
Z.1098.1
R.414.1
Z.332.1
0.95
0.9
0.85
0.8
0.75
0.75
0.8
0.85
0.9
0.95
^{207}Pb / ^{206}Pb (published)
^{207}Pb / ^{206}Pb (measured)

This is a preprint, the final version is subject to change, of the American Mineralogist (MSA)
Cite as Authors (Year) Title. American Mineralogist, in press.
(DOI will not work until issue is live.) DOI: http://dx.doi.org/10.2138/am-2017-5903

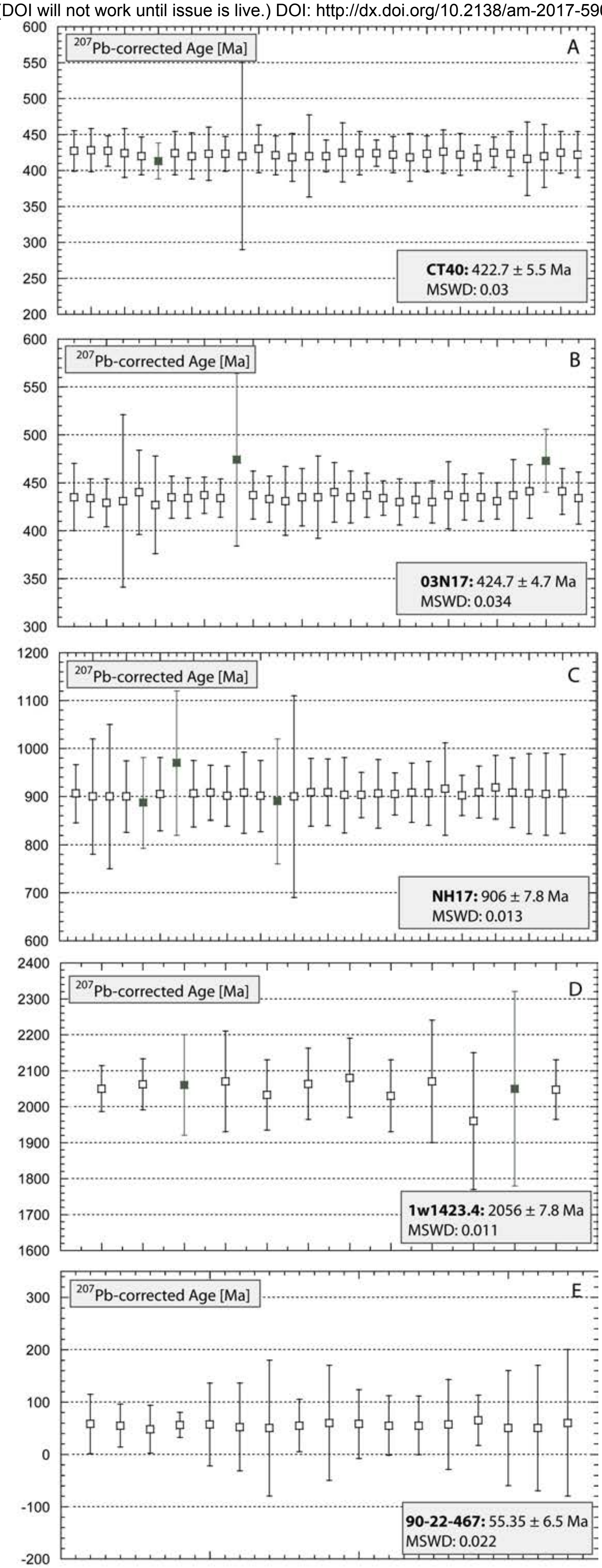

This is a preprint, the final version is subject to change, of the American Mineralogist (MSA)
Cite as Authors (Year) Title. American Mineralogist, in press.
(DOI will not work until issue is live.) DOI: http://dx.doi.org/10.2138/am-2017-5903

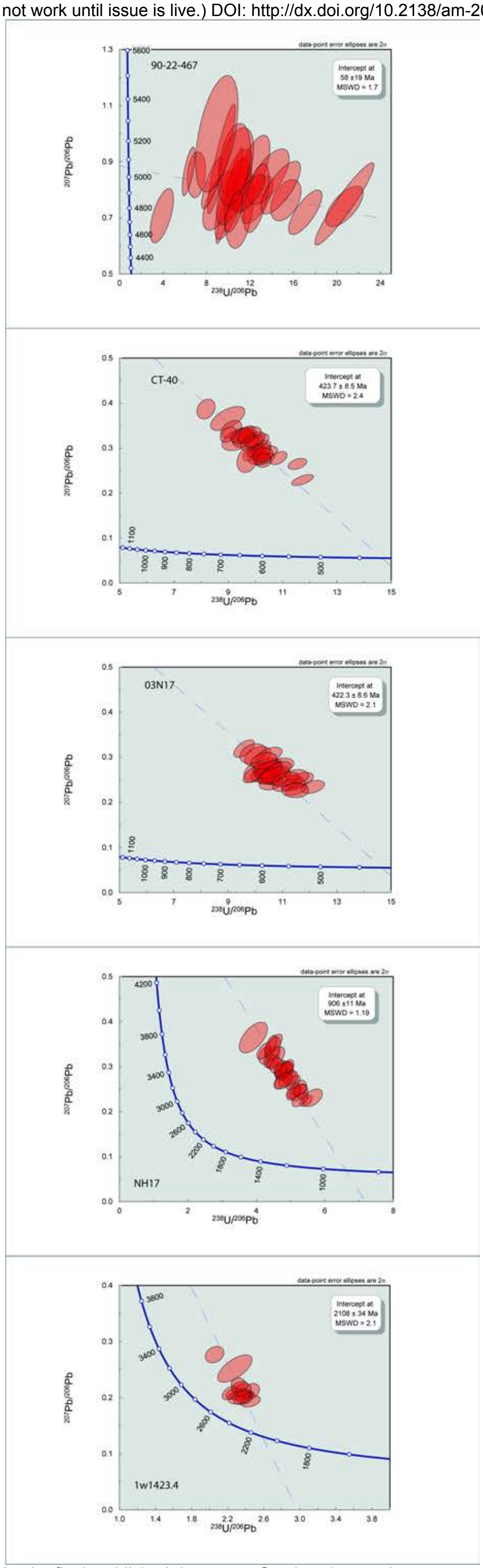

This is a preprint, the final version is subject to change, of the American Mineralogist (MSA)
Cite as Authors (Year) Title. American Mineralogist, in press.
(DOI will not work until issue is live.) DOI: http://dx.doi.org/10.2138/am-2017-5903

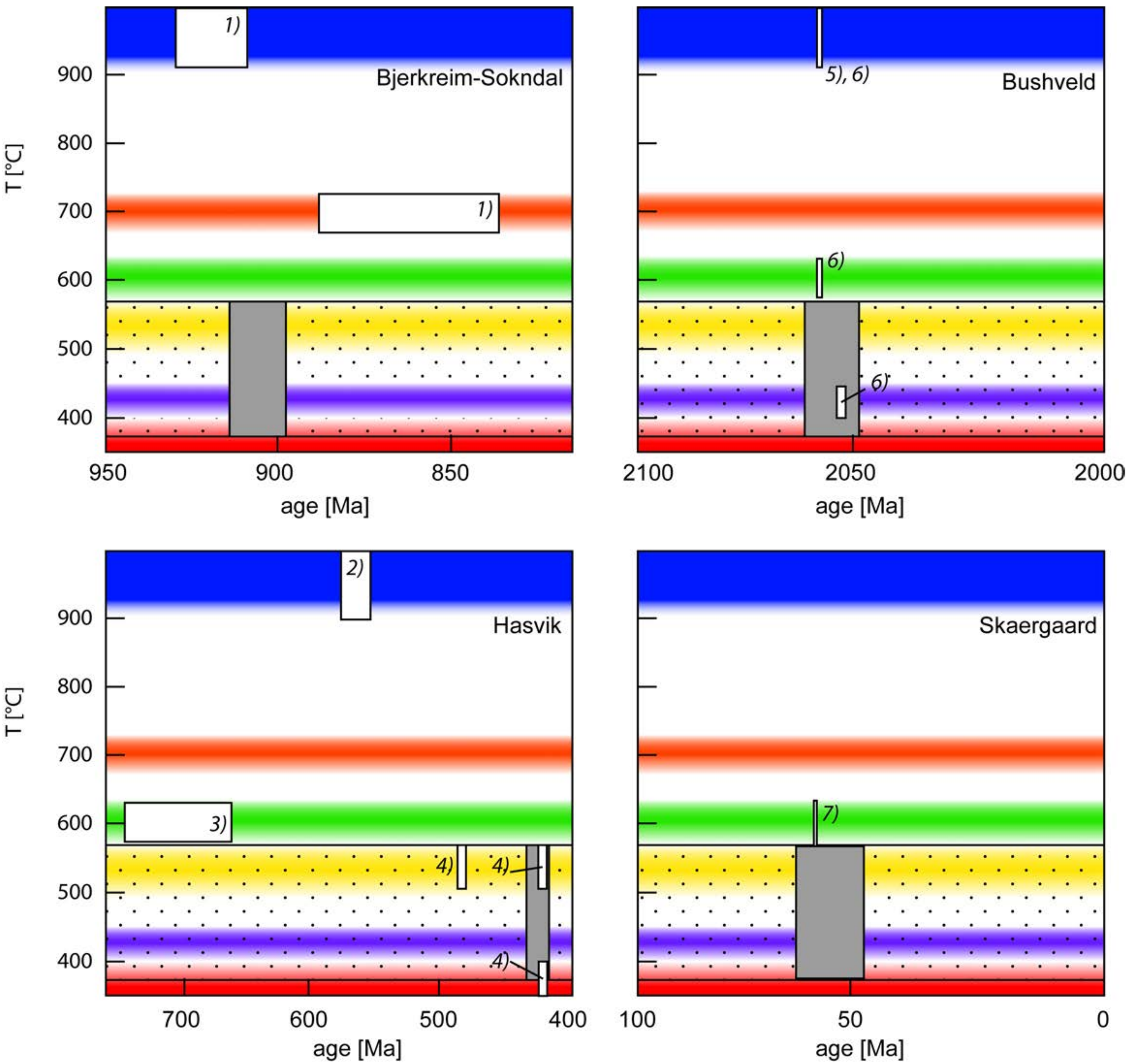

This is a preprint, the final version is subject to change, of the American Mineralogist (MSA)
Cite as Authors (Year) Title. American Mineralogist, in press.
(DOI will not work until issue is live.) DOI: http://dx.doi.org/10.2138/am-2017-5903

	Age [Ma]	initial $^{207}Pb/^{206}Pb$	reference
apatite:			
MAD2	474	0.8681	Thomsen et al. 2012
Mount McClure	523.5	0.88198	Schoene and Bowring 2006
Kovdor	377.5	0.83087	Amelin and Zaitsev 2002
Durango	31.44	0.8376	McDowell et al. 2005
feldspar:			
R.414.1	-	0.8332*	Flowerdew et al. 2012
Z.332.1	-	0.8816*	Flowerdew et al. 2012
Z.1098.6	-	0.8096*	Flowerdew et al. 2012

Table 1: Reference materials and feldspar samples applied in this study for apatite U/Pb ages and I

*PbC composition in feldspar (*calculated from published $^{207}Pb/^{204}Pb$ – $^{206}Pb/^{204}Pb$ ratios).*

This is a preprint, the final version is subject to change, of the American Mineralogist (MSA)
Cite as Authors (Year) Title. American Mineralogist, in press.
(DOI will not work until issue is live.) DOI: http://dx.doi.org/10.2138/am-2017-5903

sample	origin	age [Ma]	references
90-22-467	Skaergaard Intrusion, Greenland, Upper Zone b, Layered Series	55.96	Wotzlaw et al. 2012
CT40, 03N17	Hasvik Layered Intrusion, Norway, apatite-oxide gabbro, upper zone	562 ± 6	Tegner et al. 1999, Roberts et al. 2006
NH-17	Bjerkreim-Sokndal Intrusion, Norway, apatite-oxide gabbro, MCU III, Teksevatnet W	932 ± 5	Meyer et al. 2002
1w1423.4	Bushveld Complex, South Africa, apatite-oxide gabbro, Upper Zone c	2056.88	Scoates and Wall 2015, Tegner et al. 2006

Table 2: Samples analyzed in this study for apatite U/Pb ages and Pb isotopic composition in feldspar.

(DOI will not work until issue is live.) DOI: http://dx.doi.org/10.2138/am-2017-5903

NWR-193 nm excimer laser ablation system:	
Energy density	7 J cm^{-2}
Spot size apatite	50 μm
Spot size and stage speed feldspar	150 μm, 5 μm s^{-1}
Repetition rate apatite	10 Hz
Repetition rate feldspar	20 Hz
He carrier gas	500 ml min^{-1}
Thermo XSeries2 quadrupole ICP-MS:	
Forward power	1400 W
Nebulizer gas flow	0.92 l min^{-1}
Cooling gas	13 l min^{-1}

Table 3: Instrumental parameters and analytical conditions of the LA-ICP-MS system applied for qua

This is a preprint, the final version is subject to change, of the American Mineralogist (MSA)
Cite as Authors (Year) Title. American Mineralogist, in press.
(DOI will not work until issue is live.) DOI: http://dx.doi.org/10.2138/am-2017-5903

ntitative analyses .

(DOI will not work until issue is live.) DOI: http://dx.doi.org/10.2138/am-2017-5903

Dwell times [ms] (set 1)	^{43}Ca (5), ^{202}Hg (40), ^{204}Pb,Hg (50), ^{206}Pb (50), ^{207}Pb (80), ^{208}Pb (40), ^{232}Th (40), ^{238}U (50), ^{248}ThO (20)
Dwell times [ms] (set 2)	^{43}Ca (5), ^{202}Hg (20), ^{204}Pb,Hg (25), ^{206}Pb (100), ^{207}Pb (120), ^{208}Pb (20), ^{232}Th (20), ^{238}U (50), ^{248}ThO (20)
Dwell times [ms] (set 3)	^{43}Ca (5), ^{202}Hg (20), ^{204}Pb,Hg (25), ^{206}Pb (120), ^{207}Pb (160), ^{208}Pb (15), ^{232}Th (10), ^{238}U (45), ^{248}ThO (20)

Table 4: Instrument dwell times for U/Pb geochronology of apatite.

		Durango	MM	Kovdor
	published age	31.44	523.5	377.5
method 1	age	31.2	524	377
	error	3.9	13	5.7
	accuracy %	-0.76	0.1	-0.13
	precision %	12.5	2.48	1.51
method 2	age	32.4	523.3	377.8
	error	2.7	4.3	6
	accuracy %	3.05	-0.04	0.08
	precision %	8.33	0.82	1.59
method 3	age	31.42	523.2	378.5
	error	0.81	4.1	4
	accuracy %	-0.06	-0.06	0.26
	precision %	2.58	0.78	1.06

Table 5: ^{207}Pb-corrected ages for apatite reference materials analyzed as unknowns.

	measured	published	deviation (%)
Z.332.1	0.8750 ± 0.017	0.8816 ± 0.0001	0.75
Z.1098.6	0.8091 ± 0.009	0.8096 ± 0.0001	0.06
R.414.1	0.8267 ± 0.008	0.8332 ± 0.0001	0.78

Table 6: $^{207}Pb/^{206}Pb$ ratios of the pre-analyzed samples in comparison with published values and t

he deviation of measured from published values in %.

	Intrusion	$^{207}Pb/^{206}Pb$ feldspar	$^{207}Pb/^{206}Pb$ S & K	published age [Ma]	207Pb age feldspar [Ma]	207Pb age S & K [Ma]	intercept age feldspar [Ma]	intercept age S & K [Ma]
90-22-467	Skaergaard	0.8851	0.8387	55.960 ± 0.018	55.35 ± 6.5	55.69 ± 5.9	58 ± 19	35 ± 14
CT-40	Hasvik	0.8323	0.8614	562 ± 6	422.7 ± 5.5	422.6 ± 5.8	423.7 ± 8.5	432.6 ± 5.4
03N17	Hasvik	0.8311	0.8626	562 ± 6	424.7 ± 4.7	434.5 ± 6.1	422.3 ± 8.6	432.6 ± 5.2
NH-17	Bjerkreim-Sokndal	0.8716	0.897	932 ± 5	906.0 ± 7.8	907.7 ± 8.0	906 ± 11	904.7 ± 8.1
1w1423.4	Bushveld	1.0029	1.0059	2056.88 ± 0.41	2056.0 ± 7.8	2056.2 ± 9.0	2108 ± 34	2109 ± 33

Table 7: $^{207}Pb/^{206}Pb$ ratios from feldspar analyses and from Stacey and Kramers Pb evolution model (S & K) with corresponding ^{207}Pb-corrected ages and intercepot ages of analyzed apatite samples

	apatite			feldspar	
	^{206}Pb (cps)	^{207}Pb (cps)	^{238}U (cps)	^{206}Pb (cps)	^{207}Pb (cps)
Mount McClure	3000	690	29000	-	-
90_22_467	167	131	2000	2200	1900
CT_40	730	208	3500	5200	4310
03N17	1170	390	11400	17500	14600
NH_17	700	181	7400	7400	6500
1W14234	2450	540	5800	7000	7100

Table 8: Raw count rates in counts per second (cps) for 206Pb, 207Pb, and 238Uin apatite and

feldspar.